AIMS Materials Science, 12(5): 944–964.
DOI: 10.3934/matersci.2025042
Received: 02 July 2025
Revised: 01 September 2025
Accepted: 04 September 2025
Published: 16 September 2025

https://www.aimspress.com/journal/Materials

Research article

Impact of feed rate, speed, and fiber orientation on drilling quality in coir epoxy composites

K B Vinay[1], B T Ramesh[2,*], D S Rakshith Gowda[1], Sur Anirban[2] and G V Naveen Prakash[1]

[1] Vidyavardhaka College of Engineering (VTU, Belagavi), Mysuru-570002, Karnataka, India
[2] Symbiosis Institute of Technology (SIT), Symbiosis International (Deemed University) (SIU), Lavale, Pune 412115, Maharashtra, India

* **Correspondence:** Email: rameshbt049@gmail.com; Tel: +91-9-900-784-915.

Abstract: Coir fiber–reinforced epoxy composites are increasingly used in sustainable applications such as construction materials and furnishings. However, drilling these natural fiber composites poses challenges, including delamination, poor surface finish, and dimensional inaccuracies. This study evaluates the effects of feed rate, spindle speed, fiber orientation, and drill diameter on machining time, surface roughness, and hole circularity during drilling of coir–epoxy composites. Specimens were fabricated via hand lay-up with fibers oriented at 0, 45, and 0 + 90°, and characterized for tensile strength following ASTM standards. A Taguchi L27 orthogonal array was employed to design experiments, with analysis of variance (ANOVA) used to quantify parameter significance. Results indicate that spindle speed significantly influences machining time and surface roughness, while drill diameter and fiber orientation primarily affect hole circularity. Notably, the 0 + 90° orientation demonstrated the highest tensile modulus (1.011 GPa). Optimized drilling conditions for minimal machining time included 0° orientation, 0.125 mm/rev feed rate, 1160 rpm spindle speed, and 6 mm drill diameter. Superior surface finish was achieved at 0° orientation, 1.25 mm/rev feed, and 580 rpm speed, whereas optimal circularity required 0/90° orientation and an 8 mm drill. These findings provide new insights into the machining behavior of coir-reinforced composites and establish parameter guidelines to enhance drilling performance and dimensional accuracy in sustainable composite manufacturing.

Keywords: machining time; surface roughness; circularity; ANOVA; Taguchi; Minitab

Abbreviations: MT: Machining time; FR: Feed rate; Ra: Surface roughness; C: circularity; D: Diameter of drill bit

1. Introduction

Natural fiber–reinforced polymeric composites have been advanced globally by concerns about plastic pollution, sustainability, and the need for high-performance materials in contemporary industries [1]. Natural fiber has numerous technological and environmental advantages for usage in polymer composites. Many natural fiber types have been studied for usage in plastics, including coir, sugarcane, bamboo, flax, wood, hemp, jute, sisal, barley, wheat, and sisal, with matrix materials classified as thermosets, thermoplastics, and elastomers [2]. One viable option for the efficient use of renewable resources, maintaining a sustainable environment, is the use of plant-derived materials in the preparation of polymer composites. Composite materials that are sustainable, lightweight, recyclable, and degradable are desired by the car industry. Natural fiber composites have found extensive applications in recent decades [3]. Because of this, scientists and researchers are focusing increasingly on using natural fibers and other plant-based resources to prepare and produce composites made of wood plastics, natural fiber polymer composites, etc. Many plant resources are used in research and in the commercial manufacture of various environmentally acceptable composites [4]. Jayashree compared the mechanical behavior of epoxy resin composites reinforced with glass fiber and jute, hemp, and sisal fibers, and found that jute and carbon-reinforced composites yielded better results, almost comparable in the test conducted as per ASTM 638-2014 procedures [5]. Coir is obtained from the husks or outer layer of coconuts, commonly seen in the tropical regions of Indonesia, the Philippines, Brazil, and India, and may be used in place of synthetic composites as reinforcement [6]. Like other natural fibers, it offers several benefits over synthetic alternatives, including low density, a cheap cost, high degree of flexibility, non-toxicity, biodegradability, and recycling [7]. According to reports, among the typical natural fibers, coir fiber has the maximum elongation at break and can withstand 4–6 times more strain than other fibers [8–10]. Materials such as carpets, ropes, mats, and fiber-reinforced plastic composites (FRPC) are among the products that often use coir fiber. The primary component of coir is a multicellular fiber with a cross-section made up of 30–300 cells. Fibre reinforced polymers (FRP) are used in the oil and natural gas production industry for several pipeline activities. It is also often used in situations when the fluids being used are highly corrosive [11]. The crystalline cellulose found in coir is helically organized inside a non-crystalline cellulose–lignin complex matrix [12]. Epoxy resin is a thermosetting plastic used in adhesives, coatings, electronic materials, and FRPC matrices [13]. Epoxy resin composites (ERCs) reinforced with coir provide new possibilities for the creation of sustainable products. The transition from synthetic materials to natural fiber–reinforced materials was advanced by these materials [14]. Furthermore, it was shown that the manufacturing process of natural fiber composites yields a noteworthy economic benefit on a weight basis, while simultaneously requiring less energy and gas emissions [15]. Researchers utilized the injection molding technique to fabricate sisal, banana, and bagasse–reinforced polymer composites and compression molding to create kenaf fiber–reinforced epoxy composites. Most researchers utilized hand lay-up techniques to fabricate FRPC, obtaining good impact strength [16,17]. To obtain consistent resin dispersion and desired thickness, hand lay-up is the best and cheapest technique available [18]. Drilling is one of the most used machining techniques to join structural components made by FRPC, because of their multi-layered structure, hybridization, and

inclusion of elements in many phases, FRPC often exhibits heterogeneity. In drilling operations, frequent issues such as delamination, fuzzing, buckling, cracking, and matrix and fiber burning happen. To mitigate these damages, a few innovative geometries, including parabolic, brad center, tripod, and web thinned, among others, were investigated [19]. The orientation of the fiber in the matrix phase also affects the mechanical behavior of the composites, which, in turn, affects the quality of the machining to some extent [20]. Drill materials affect the drilling of FRPC in terms of delamination, circularity, and cylindricity errors [21]. However, drilling process parameters, such as speed, feed rate, and drill diameter, affect the quality of drilling in terms of surface roughness (Ra) and material removal rate (MRR) [22]. The most practical and straightforward approach to assessing how process factors affect drilling quality is the Taguchi technique [23–25]. According to a survey, very few researchers have tried to investigate how natural fiber, namely, coir-reinforced epoxy resin composites, behave during drilling. Mitigating the damage caused during FRPC drilling and investigating the influence of process parameters on the quality characteristics of drilling paves the way to better-quality components, which is critical in mechanical and material engineering applications. The present study strives to address the issue by evaluating the effect of the three variables, namely, drill bit diameter, spindle speed, and feed rate, on the circularity and Ra in the drilling of epoxy resin composites reinforced with coir in different orientations. The current study addresses a gap by considering untreated coir, which is relatively underexplored, especially in structural applications. The global scenario has shifted toward the use of sustainable and biodegradable materials in the automotive industry, civil structures, and even textiles. Sanjita Wasti et al. showed that the cumulative energy demand and greenhouse gas emissions from coir-reinforced composites are much lower than those of glass fiber–reinforced composites [26]. The novelty of this work lies in investigating the coupled effects of the drilling process parameters and fiber orientation on the quality of the hole, linking them with the strength of the fiber, thus achieving the optimal solution using Taguchi's statistical approach validation for the drilling of sustainable composites suitable for structural components. The work is carried out in different phases, starting with the preparation of the coir-reinforced epoxy composites using the hand lay-up method, followed by composite testing for tensile strength, which will then be linked to the performance characteristics of the drilling. The control factors under study, including the machining drilling parameters, are decided based on expert advice and literature surveys. Experiments will be planned based on Taguchi's standard orthogonal array. Drilling will be performed on the composites for the various combinations of parameters given by the orthogonal array; for each hole, the machining time will be recorded, followed by the measurement of circularity and surface roughness. The effect of each parameter on the output responses is investigated, and an optimized combination will be drawn using Taguchi's approach and ANOVA.

2. Materials and methods

2.1. Preparation of the composite material

In the present study, epoxy resin (Lapox L12) was used as the matrix, together with hardener K6 and untreated natural coir as the reinforcement. The untreated herbal coir, a biodegradable fiber extracted from coconut husk, is known for its low density with good tensile strength and eco-friendliness. It has been explored as a sustainable reinforcement material in polymer composites. L12 is a clear, viscous epoxy resin broadly used for composite packages because of its superb mechanical and

adhesive properties and electrical and chemical resistance. At room temperature, when combined with Hardener K6, a low-viscosity hardener, the mixture yields an inflexible thermoset matrix. This epoxy-hardener gadget is specifically appropriate for embedding herbal fibers like coir, offering advanced structural integrity and environmental compatibility in composite materials. Technical specifications are given in the Atul Ltd. product catalog of the Lapox L12 and hardener K6, and shown in Tables 1 and 2, respectively.

Table 1. Technical specifications of Lapox L12.

Properties	Units	Test methods	Values	Manufacture details
Appearance	-	Visual	Clear, viscous liquid	Atul Ltd., Atul, Valsad District, Gujarat, 396020, India Manufacturing date: Aug 2024
Color	GS	ASTM D1544	Max 1	
Viscosity at 25 °C	m Pas	ASTM D2196	9000–12,000	
Epoxy value	Eq/kg	ASTM D1652	5.26–5.55	
Density at 25 °C	g/cm^3	ISO 1183	1.1–1.2	

Table 2. Technical specifications of hardener K6.

Properties	Units	Test methods	Values	Manufacture details
Appearance	-	Visual	Clear liquid	Atul Ltd., Atul, Valsad District, Gujarat, 396020, India
Viscosity at 25 °C	m Pas	ASTM D2196	5–20	
Density at 25 °C	g/cm^3	ISO 1183	0.95–1.10	

Composite materials were prepared using a mold size of 100 × 100 × 20 mm by the hand lay-up method [27,28]. 250 and 100 mL beakers were utilized for measuring and mixing the epoxy resin and hardener in the required proportions; these beakers provided accurate volume measurements and facilitated uniform mixing of the components. Epoxy resin was reinforced with untreated natural coir in three different orientations, i.e., 0, 45, and 0 + 90°, as shown in Figure 1. The average diameter of the coir is 0.10 mm, measured in a video measuring machine, and its length is 100 mm. The volume of each coir fiber was calculated as the volume of a cylinder and obtained as 0.785 mm^3. The volume fraction of the fiber was determined to be 0.37. To investigate the strength of the composites, tensile specimens were prepared as per the ASTM 3039 standard [29], as shown in Figure 2. Technical specifications of the ASTM standard are mentioned in Table 3.

Figure 1. Epoxy composites reinforced with coir in 0, 0 + 90, and 45° orientations.

Figure 1 shows epoxy resin composites reinforced with natural coir fiber in three different orientations i.e. 0 (horizontal orientation), 45, and 0 + 90° (horizontal + vertical orientation).

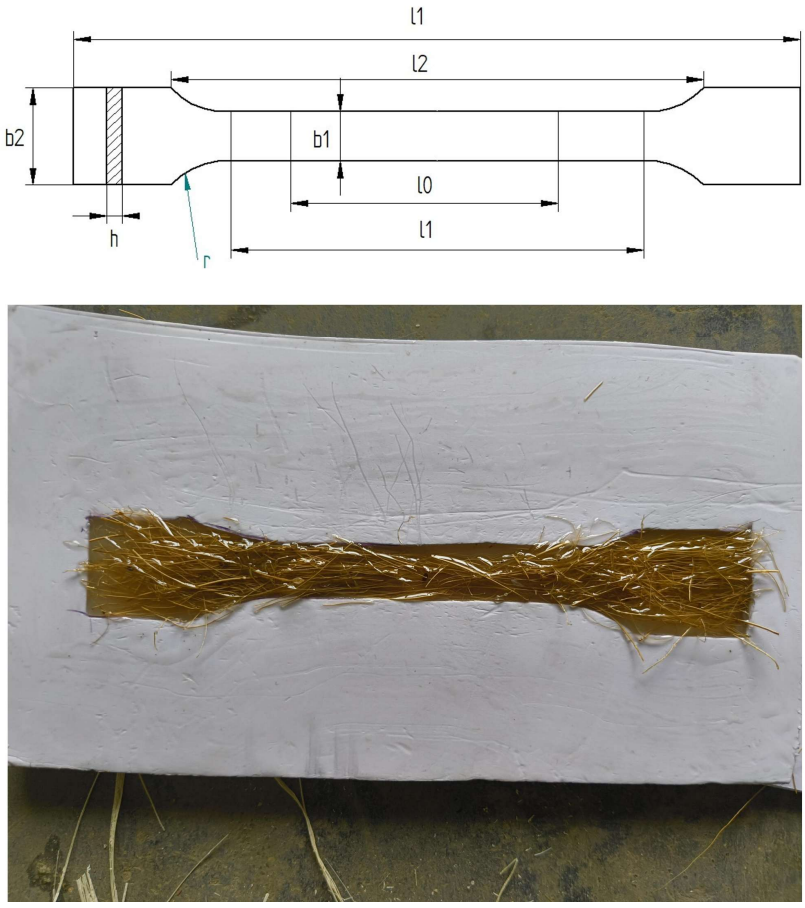

Figure 2. Tensile specimens of the composites as per the ASTM 3039 standard.

Figure 2 depicts a preparation of tensile specimen of a coir fiber–reinforced epoxy composite in agreement with the ASTM D3039 standard, used for measuring the tensile properties of polymer matrix composites.

Table 3. Technical specifications of the ASTM standard.

Symbol	Name	Dimensions in mm
l3	Overall length a	150
l1	Length of narrow parallel-sided portion	60.5
r	Radius b	60
b2	Width at end	20.1
b1	Width of the narrow portion	10.2
h	Thickness	2
L0	Gauge length	50
L	Initial distance between grips	115

2.2. Testing of the mechanical properties

To evaluate the mechanical properties of the ASTM-fabricated composites, a tensile test was performed using a Universal Testing Machine (UTM), as shown in Figure 3. This test measures the material's strength and stiffness by applying a gradually increasing pulling force until the composite fractures. The UTM records the force and the corresponding elongation (strain) of the composite throughout the test. This data is then used to calculate key tensile properties like tensile strength (maximum force before fracture) and Young's modulus (stiffness).

Figure 3. Tensile properties testing of composite specimens using UTM.

2.3. Drilling of the composite materials

An automated radial drilling machine (HMT-RM32) with a spindle speed range of 40–1800 rpm and vertical and horizontal travel of 1325 and 1420 mm, respectively, was used to drill the fabricated composites using high-speed steel (HSS) drill bits, as shown in Figure 4.

Figure 4. Automatic radial drilling machine.

The control factors and their levels considered for the study are mentioned in Table 4. Drilling experiments were performed based on Taguchi's L27 standard orthogonal array, selected for four control factors and three levels in Minitab software. Machining time (MT) for each run was recorded using a stopwatch.

Table 4. Control factors and their levels.

Factors	Unit	Level 1	Level 2	Level 3
Feed rate (FR)	mm/rev	0.125	0.687	1.25
Spindle speed (S)	rpm	300	580	1160
Coir orientation (CO)	°	0	45	0 + 90
Diameter of drill (D)	mm	6	8	10

Table 4 outlines the control factors and their corresponding levels used in the experimental study, likely related to drilling or machining of coir fiber–reinforced epoxy composites. The four key factors considered are:

- Feed rate (FR) in mm/rev, with levels 0.125, 0.687, and 1.25.
- Spindle speed (S) in rpm, with levels 300, 580, and 1160.
- Coir orientation (CO) in degrees, set to 0, 45, and a combination of 0 + 90°.
- Drill diameter (D) in mm, with sizes 6, 8, and 10 mm.

These factors and levels are critical for analyzing the influence of machining parameters on drilling performance, including aspects like thrust force, delamination, and surface finish, especially in natural fiber–reinforced composites. Drilling was performed for the different combinations of factors in each run, given by a standard orthogonal array. The Ra and C of each hole were measured using Surfcom Flex 50-A and a digital profile projector, as shown in Figures 5 and 6, respectively.

Figure 5. Measurement of Ra using the Surfcom Flex 50-A.

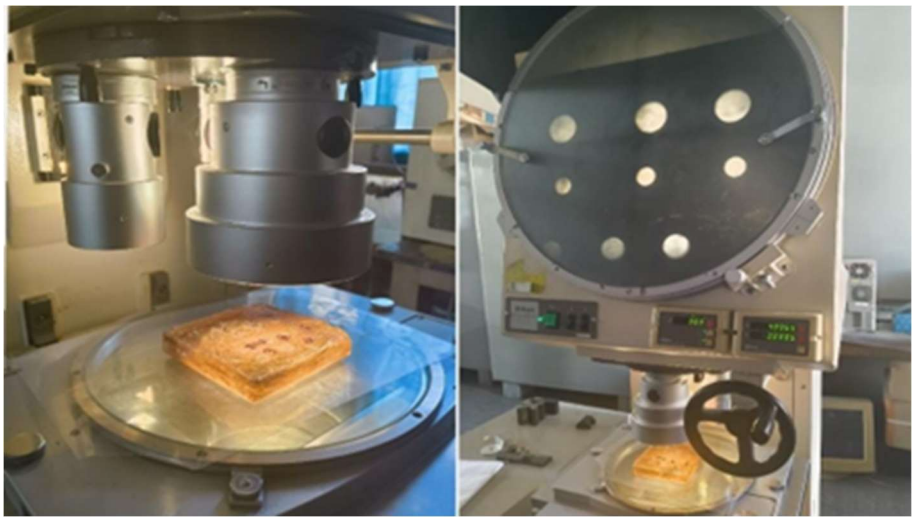

Figure 6. Measurement of circularity using a digital profile projector.

3. Results and discussion

3.1. Analysis of tensile properties

Figure 7 shows coir fiber–strengthened epoxy composite specimens after tensile testing. Visible signs and symptoms of fractures and fiber pull-out can be observed on the slim gauge sections, indicating failure underneath the axial load. The different fracture styles relate to different fiber orientations and cargo distribution throughout the samples. These effects provide insights into the mechanical conduct, power, and stiffness of the composites and help to examine the effectiveness of fiber-matrix bonding under tensile strain.

Figure 7. Composite specimens after tensile test.

Table 5. Results of the tensile test.

Particulars	Unit	Value		
		0°	45°	0 + 90°
Modulus	GPa	1.001	0.26	1.011
Limits of proportionality	MPa	1.448	2.562	1.648
Strain at maximum load	%	1.15	4.298	1.351
Stiffness	kN/mm	0.534	0.173	0.674

The tensile test results, detailed in Table 5, show that the epoxy resin composite with 45° yielded the highest strain percentage at a maximum load of 4.298%, a superior stiffness of 0.173 kN/mm, and a notable limit of proportionality, while exhibiting the lowest modulus. The composite with a 0 + 90° coir orientation demonstrated reduced elasticity compared to the 45° orientation but higher than the 0° orientation, together with a middle value of strength. The composite with a 0° coir orientation demonstrated diminished elasticity in comparison with the other orientations, also having the lowest strength. This comprehensive analysis underscores the critical influence of coir orientation on material properties.

3.2. Analysis of drilling experimental results

The experimental results, based on the Taguchi L27 orthogonal array, are shown in Table 6. The composite materials after the drilling operation are shown in Figure 8. Table 6 highlights the different combinations of drilling process parameters. The inherent heterogeneity of the natural fiber, which is a result of the variable matrix–fiber interfacial bonding and fiber orientation, causes the obvious deviation in the expected drilling responses, as is evident in Table 6. The best output responses with respect to the drilling process parameters are summarized in Table 7.

Figure 8. Composite materials after drilling operation.

Table 6. Experimental results.

Runs	FR	S	CO	D	MT (s)	Ra (μm)	C (mm)
1	0.125	300	0	6	14.6	7.682	0.04
2	0.125	300	45	8	19.82	4.364	0.01
3	0.125	300	0 + 90	10	19.57	6.646	0.023
4	0.125	580	0	8	9.60	7.289	0.013
5	0.125	580	45	10	9.98	4.619	0.015
6	0.125	580	0 + 90	6	8.98	2.102	0.008
7	0.125	1160	0	10	4.23	4.866	0.03
8	0.125	1160	45	6	4.64	6.357	0.01
9	0.125	1160	0 + 90	8	4.7	6.79	0.005
10	0.687	300	0	8	27.57	3.471	0.003
11	0.687	300	45	10	26.92	4.641	0.005
12	0.687	300	0 + 90	6	28.73	3.611	0.001
13	0.687	580	0	10	16.4	4.443	0.01
14	0.687	580	45	6	15.13	6.999	0.047
15	0.687	580	0 + 90	8	53.97	4.887	0.01
16	0.687	1160	0	6	7.11	6.436	0.065
17	0.687	1160	45	8	7.59	6.748	0.01
18	0.687	1160	0 + 90	10	7.78	3.827	0.036
19	1.25	300	0	10	43.46	2.643	0.01
20	1.25	300	45	6	43.38	4.826	0.029
21	1.25	300	0 + 90	8	45.35	5.212	0.013
22	1.25	580	0	6	22.11	1.647	0.01
23	1.25	580	45	8	25.93	3.858	0.01
24	1.25	580	0 + 90	10	23.67	2.864	0.06
25	1.25	1160	0	8	11.51	6.206	0.02
26	1.25	1160	45	10	12.76	14.701	0.028
27	1.25	1160	0 + 90	6	12.48	9.32	0.0055

Table 7. Summarized experimental results.

Response	Best run No.	Feed rate (mm/rev)	Spindle speed (rpm)	Orientation	Drill dia. (mm)	Value
Machining time (MT)	7	0.125	1160	0°	10	4.23 s
Surface roughness (Ra)	22	1.25	580	0°	6	1.647 μm
Circularity (C)	12	0.687	300	0+90°	6	0.001 mm

3.2.1. Effect of control factors on machining time

Table 6 indicates a moderately positive relationship between FR and MT. This implies that an increase in feed rate leads to a corresponding increase in machining time, although the relationship is not strictly linear. The maximum machining time observed was 53.77 s at the 15th run, where FR and S were at a moderate level; the drill diameter was 8 mm, and the coir was reinforced at 0 and 90°. This is because at the 0 + 90° orientation, more time is taken by the drill bit to penetrate the work material. The lowest machining time was 4.23 s, with FR at its lowest level and S at its highest level. It is clear that an increase in S results in a reduction in MT. Orienting the coir at 0° resulted in the lowest MT. However, the D alone does not have a significant effect on MT.

3.2.2. Effect of control factors on surface roughness

The lowest Ra observed was 2.102 μm at the 22nd run, where the FR was at the highest level, S was at a moderate level, the orientation of the coir was 0°, and D was 6 mm. The highest Ra observed was 14.701 μm at the 26th run, where both FR and S were at high levels, the orientation of the coir was 45°, and D was 10 mm. When the average Ra is considered, an FR of 0.687 mm/rev yielded the lowest value. There was no significant difference between the Ra at higher and lower levels of FR. As the S increases from 300 to 580 rpm, Ra is reduced to a small extent. Further increases in S, from 580 to 1160 rpm, deteriorate the surface, with a larger value of Ra because of the combined effect with FR. Lower values of Ra are obtained with the 0° coir orientation, and deteriorated Ra is observed at 45°. There is a negligible deviation in the Ra at different D values; this shows that D has no significant effect on Ra.

3.2.3. Effect of control factors on circularity

The maximum circularity observed was 0.065 mm at the 16th run, where FR was at a moderate level, S was at a higher level, the orientation of the coir was 0°, and D was 6 mm. The lowest circularity observed was 0.001 mm at the 12th run, where FR was at a moderate level, S was at the lower level, the orientation of the coir was 0 + 90°, and D was 6 mm. An increase in FR from 0.125 to 0.687 mm/rev slightly increased C; a further increase in FR to 1.25 mm/rev reduced C to a negligible amount. Table 5 clearly shows that the increase in S has adverse effects on C. A larger value of C was the result of maximum speed. C was acceptable at low levels of S. The orientation of the coir in epoxy resin did not have much effect on C. However, C was better at a 0 + 90° coir orientation compared to the other orientations, and was consistent at 45° orientation. A better C was observed at D of 8 mm, and there was a negligible difference in the variation of C at D of 6 and 10 mm.

3.3. Optimization of process parameters using Taguchi's technique

An optimized run was determined for MT, Ra, and circularity using Taguchi's technique, using the Minitab software based on the *smaller is better* condition.

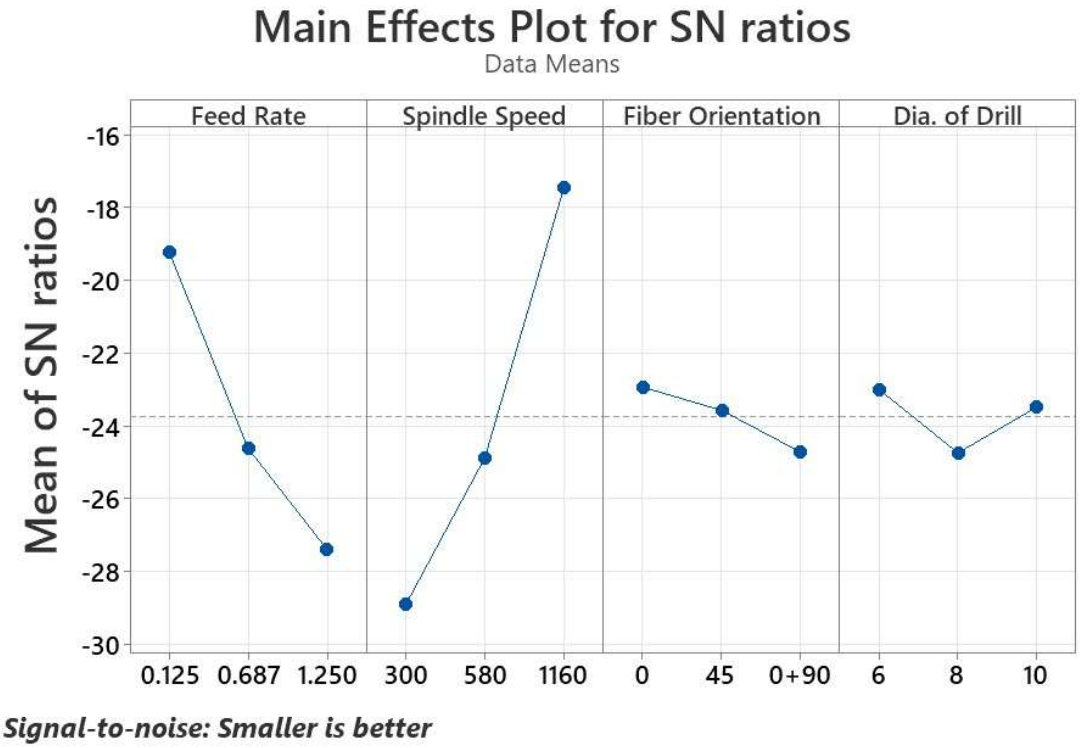

Figure 9. Main effects plot for SN ratios for the machining time.

Based on the comprehensive analysis of the 27 combinations proposed by the Taguchi technique, as delineated in Table 5, the graph presented in Figure 9 provides conclusive evidence regarding the optimal configuration for minimizing the machining time. Notably, meticulous scrutiny of the graph suggests that the combination characterized by a FR of 0.125 mm/rev, S of 1160 rpm, a 0° fiber orientation, and a D of 6 mm emerges as the most favorable. It is imperative to underscore that this determination is underpinned by the principle that smaller values are inherently preferable in this context.

The graph depicted in Figure 10 offers insights into the optimal setup for Ra. Upon meticulous analysis of the graph, it becomes evident that the configuration characterized by an FR of 1.250 mm/rev, S of 580 rpm, a 0˚ fiber orientation, and a D of 6 mm emerges as the most advantageous.

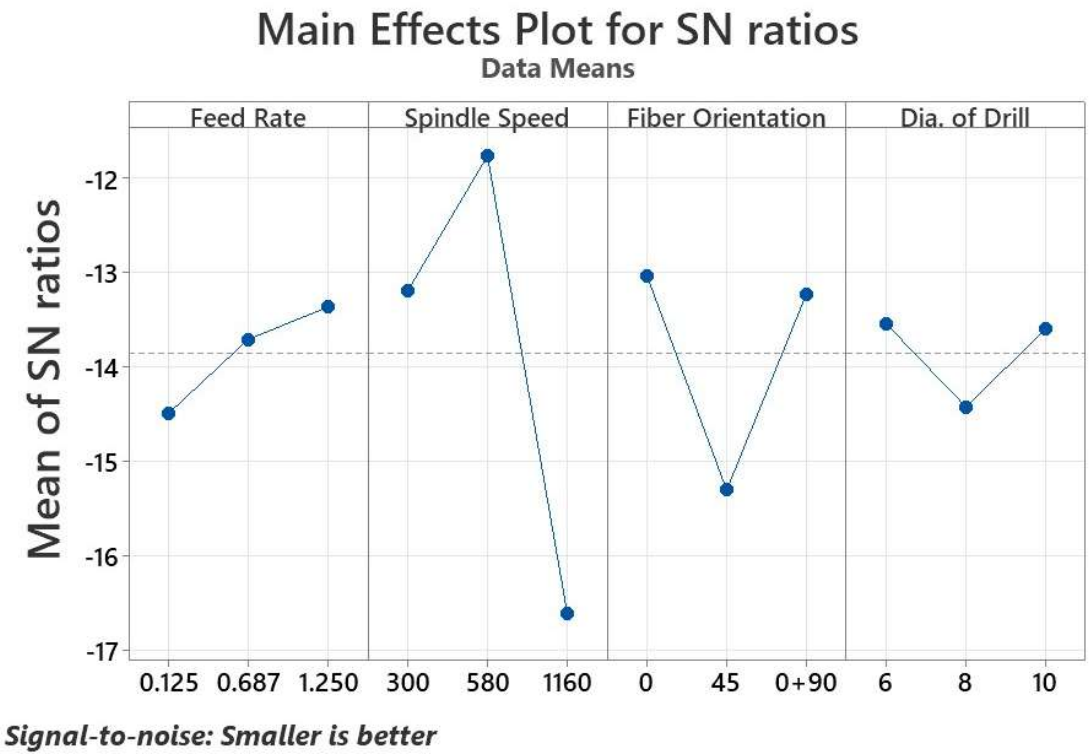

Figure 10. Main effects plot for SN ratios for Ra.

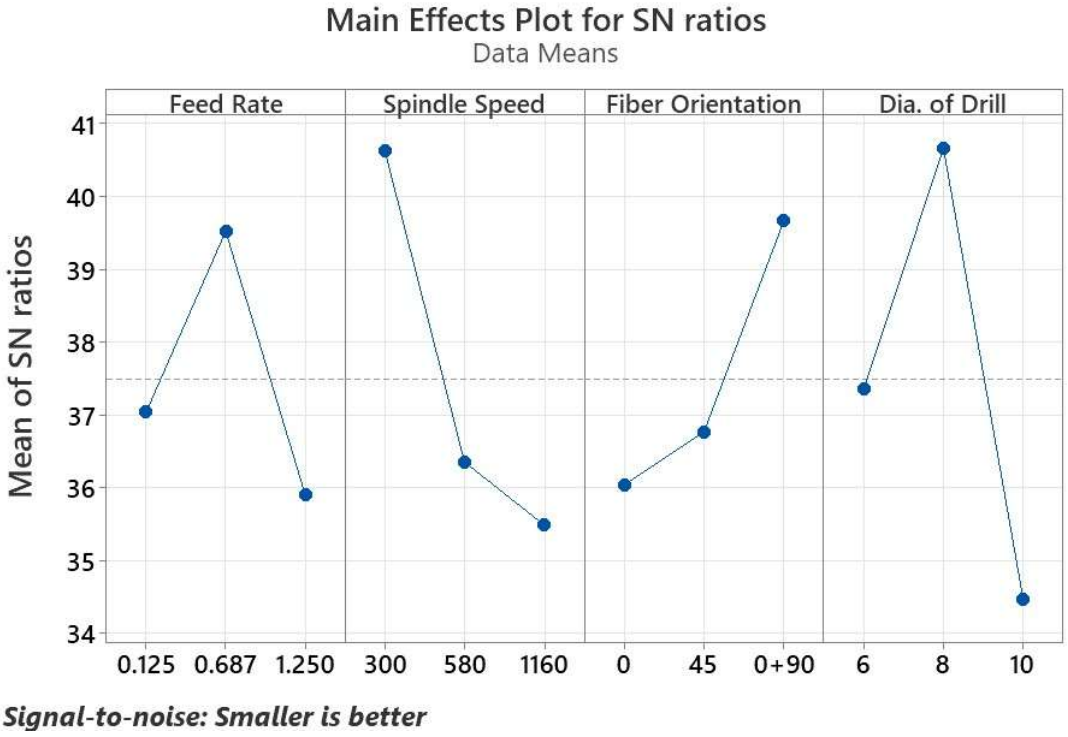

Figure 11. Main effects plot for SN ratios for circularity.

Figure 11 offers definitive insights into the optimal setup for circularity. Upon meticulous scrutiny, it becomes apparent that the configuration featuring an FR of 0.687 mm/rev, S of 300 rpm, a 0 +90° fiber orientation, and a D of 8 mm stands out as the most advantageous. It is paramount to emphasize that this determination is predicated on the fundamental tenet that smaller values hold inherent preference within this context.

3.4. Analysis of variance (ANOVA)

The ANOVA analysis yields valuable insights into the determinants of improved MT, with spindle speed emerging as the most influential factor, followed by FR, CO, and finally, D, as evidenced by their respective signal-to-noise (SN) ratio values, mentioned in Table 8. This hierarchical ranking underscores the pivotal role of spindle speed in optimizing machining efficiency, underscoring its significant impact on overall performance outcomes. Moreover, the consequential influence of FR and CO underscores the intricate interplay between process parameters and machining quality. Notably, while D ranks as the least influential parameter, its contribution remains a crucial consideration in achieving optimal machining results.

Table 8. Response table for signal-to-noise ratios of MT.

Level	FR (mm/rev)	S (rpm)	CO	D (mm)
1	–19.23	–28.92	–22.94	–23.01
2	–24.62	–24.88	–23.58	–24.75
3	–27.39	–17.45	–24.72	–23.49
Delta	8.17	11.47	1.78	1.74
Rank	2	1	3	4

Based on the examination of the normal probability graph depicted in Figure 12, and considering the complexity of our parameters encompassing three levels and four factors, a discernible departure from the anticipated probability curve is observed. This deviation warrants careful scrutiny, as it may signify potential irregularities in the machining setup. Notably, observations of spindle oscillations suggest a plausible explanation for this deviation from the expected values. Consequently, it is imperative to acknowledge the influence of such operational anomalies on the precision and reliability of the machining process. Addressing these discrepancies is paramount to ensure adherence to desired performance standards and to mitigate potential downstream effects on product quality and operational efficiency.

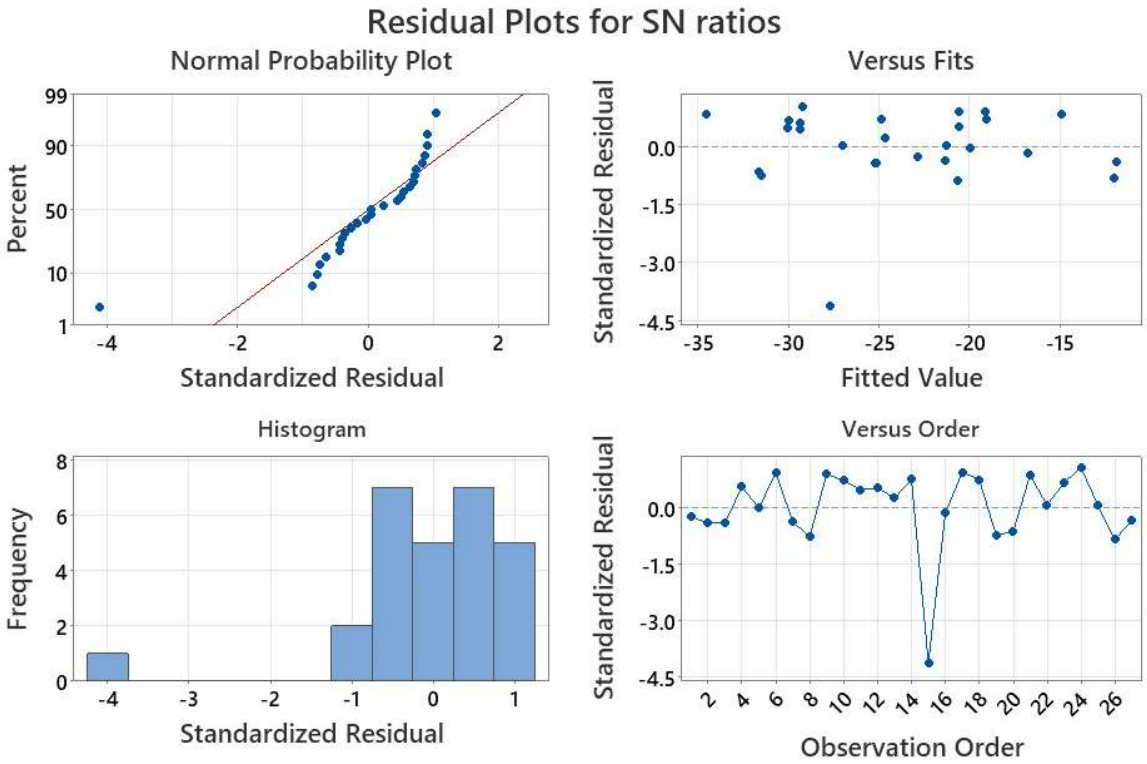

Figure 12. Residual plots for SN ratios of machining time.

The ANOVA examination in Table 9 and Figure 13 reveals spindle speed as the foremost influential factor impacting Ra, followed closely by CO, FR, and D, in descending order of significance, as discerned from their respective SN ratio values. This hierarchical arrangement underscores the paramount importance of S in governing Ra outcomes, indicating its pivotal role in shaping machining quality. Furthermore, the consequential influence of CO and FR highlights the nuanced interplay between process variables and the resultant surface finish. Although D ranks as the least influential parameter, its contribution remains integral to achieving optimal roughness characteristics. This trend is in good agreement with the influence of the spindle speed on the hole quality stated in the study by Shashi Ranjan Pathak et al., in which an increase in spindle speed increased drill temperature, which allows the drill bit to move more easily, leading to a minimum surface roughness [30].

Table 9. Response table for signal-to-noise ratios of Ra.

Level	FR (mm/rev)	S (rpm)	CO	D (mm)
1	−14.49	−13.19	−13.03	−13.54
2	−13.70	−11.76	−15.30	−14.42
3	−13.36	−16.61	−13.22	−13.60
Delta	1.13	4.85	2.27	0.88
Rank	3	1	2	4

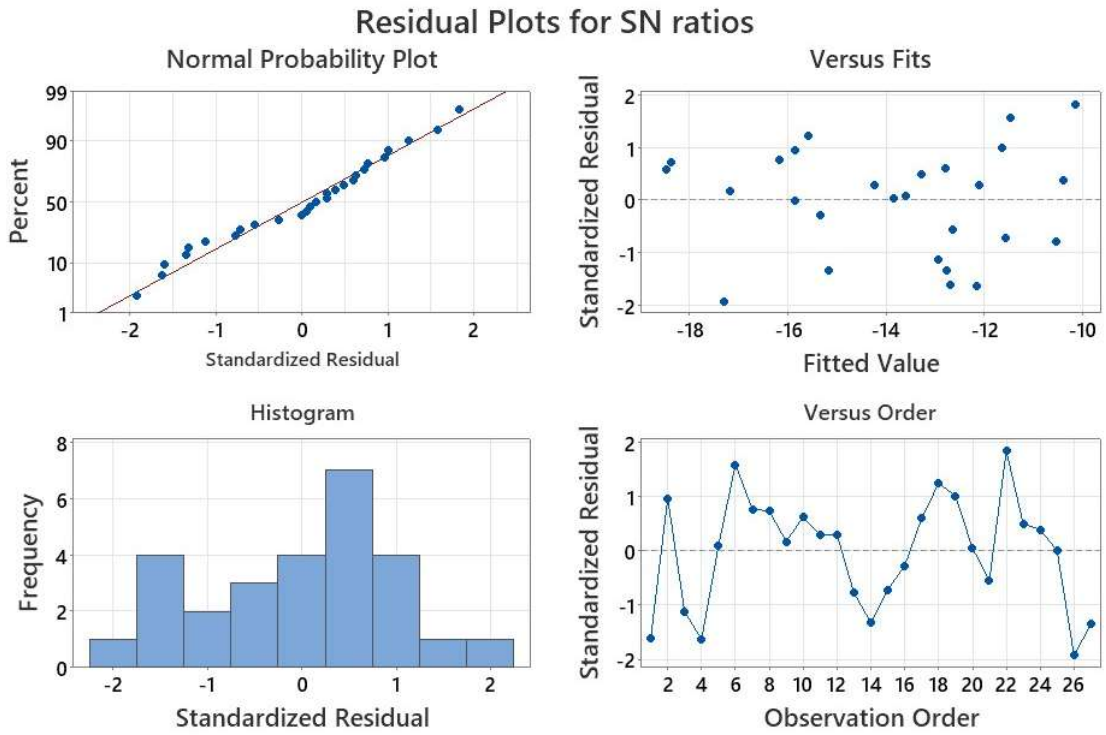

Figure 13. Residual plots for SN ratios of Ra.

Table 10. Response table for signal-to-noise ratios of circularity.

Level	FR (mm/rev)	S (rpm)	CO	D (mm)
1	37.04	40.63	36.04	37.35
2	39.52	36.35	36.76	40.66
3	35.90	35.48	39.66	34.45
Delta	3.61	5.15	3.63	6.20
Rank	4	2	3	1

Table 10 unveils D as the foremost influential factor affecting C, with S following suit, trailed by CO, and lastly, FR, in accordance with their respective SN ratio values. Remarkably, this ranking adheres to the principle that smaller values are inherently preferred for optimal C outcomes. This delineated hierarchy underscores the paramount significance of D in shaping C, affirming its pivotal role in achieving desired geometrical integrity. Furthermore, the consequential influence of S and CO underscores the nuanced interplay between machining parameters and the resultant C metrics. Although FR emerges as the least influential parameter, its careful consideration remains integral to ensuring comprehensive optimization of C standards. This insightful ANOVA-driven analysis provides a robust framework for strategic decision-making aimed at refining machining processes to achieve superior C performance. However, the observation in the current study is contrary to the work of P. Ghabezi et al., where feed rate was the most influential on the circularity, which is measured indirectly by the delamination factor [31]. However, the influence of spindle speed on the delamination factor, which decides the hole quality, is in good agreement with the observation made by Ghabezi et al. [32].

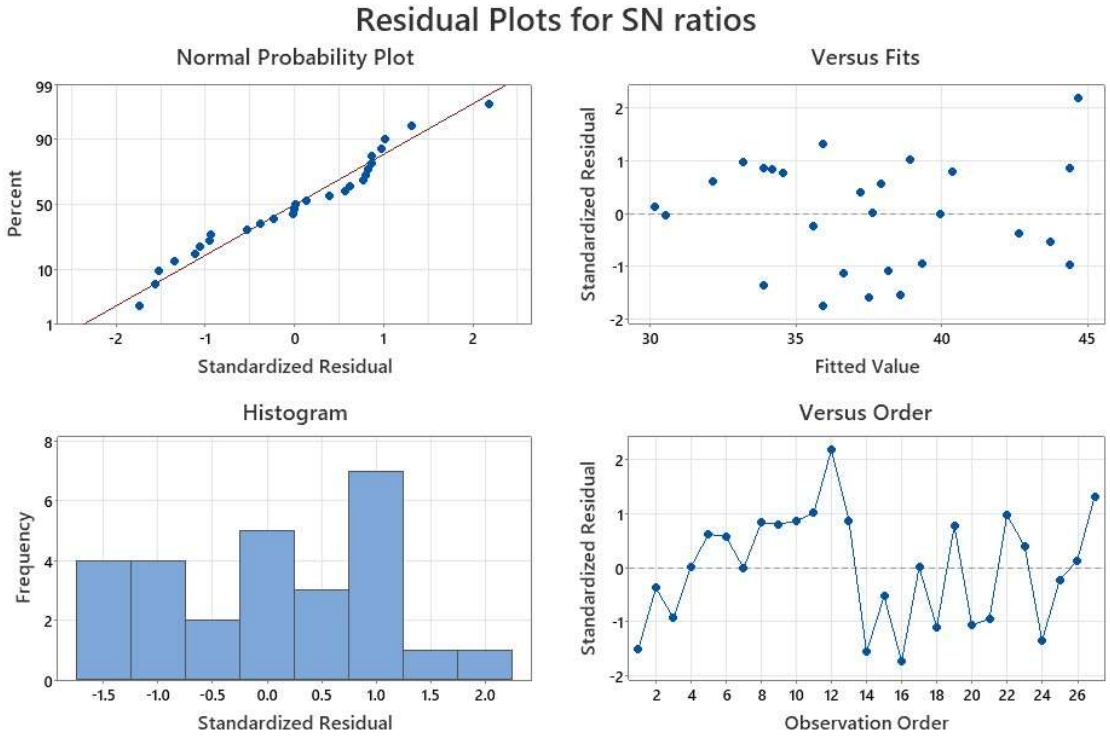

Figure 14. Residual plots for SN ratios of circularity.

Upon examination of the normal probability graph pertaining to C, as depicted in Figure 14, and taking into account our parameters characterized by three levels and four factors, a discernible yet minor deviation from the anticipated probability curve is noted. This observed variance, while present, appears notably less pronounced compared to that observed for MT and falls short of the precision observed in the case of Ra. Consequently, it can be inferred that the observed values generally align with those predicted by the graph. However, it is notable that C stands between Ra and MT in terms of the fidelity of alignment with the predicted graph, occupying a middle position in this regard. This nuanced analysis underscores the relative accuracy of the predictive model for C, albeit with room for further refinement of CO, necessitating continued vigilance and optimization efforts to enhance predictive capabilities and operational outcomes within the machining domain.

4. Conclusions

The fabrication process of epoxy resin–based polymer matrix composite involves the incorporation of reinforcing coir fibers oriented at angles of 0, 45, and 0 + 90°, facilitated by the hand lay-up method. Subsequent evaluation, analysis, and optimization of the control factors for the drilled hole show distinct performance trends across machining parameters. Based on the results and discussion, the following conclusions were made:

- The 0 + 90° fiber orientation exhibited maximum stiffness, surpassing both 0 and 45° orientations. Furthermore, this orientation excelled in modulus, registering a value of 1.011 GPa. In contrast, the 45° orientation displayed the least favorable mechanical properties, characterized by a modulus of 0.26 GPa and a stiffness of 0.173 kN/mm. Meanwhile, the 0° fiber orientation occupied an

intermediate position, with a stiffness of 0.534 kN/mm and a modulus of 1.001 GPa when compared to the other orientations.

- Spindle speed emerged as the most influential factor on machining time and surface roughness, and the drill diameter was the most significant factor on circularity.
- The 0° fiber orientation emerged as the optimal choice, with an ideal feed rate of 0.125 mm/rev, spindle speed of 1160 rpm, and drill diameter of 6 mm. Similarly, for roughness refinement, the 0° fiber orientation proved most effective, with an optimal feed rate of 1.250 mm/rev, spindle speed of 580 rpm, and drill diameter of 6 mm. Conversely, for circularity enhancement, the 0 + 90° fiber orientation demonstrated superior performance, requiring a feed rate of 0.687 mm/rev, spindle speed of 300 rpm, and drill diameter of 8 mm for optimal results.
- The results help us drawing the conclusion that even though spindle speed has a dominant effect on surface roughness, there are strong interaction between spindle speed and feed rate, i.e., a high feed rate of 1.25 mm/rev and spindle speed (580 rpm) results in the smoothest surface (Ra = 1.647 μm, run 22), whereas maximum speed (1160 rpm) leads to Ra = 14.701 μm (run 26).
- Even though spindle speed is the most influential factor on machining time, there is a significant interaction between drill diameter and speed, influencing the machining time (53.97 s).

Use of AI tools declaration

The authors declare they have not used Artificial Intelligence (AI) tools in the creation of this article.

Acknowledgments

The research was funded by AICTE under RPS scheme.

Author contributions

Vinay K B: investigation, data curation, validation, writing–original draft; Ramesh B T: resources, experimental support, data curation; Rakshith Gowda D S: conceptualization, methodology, supervision, writing–review & editing; Anirban Sur: formal analysis, visualization, writing–review & editing; Naveen Prakash G V: software, statistical analysis, visualization, writing–original draft support.

Conflict of interest

The authors declare no conflict of interest.

References

1. Soni A, Das PK, Gupta SK, et al. (2024) An overview of recent trends and future prospects of sustainable natural fiber-reinforced polymeric composites for tribological applications. *Ind Crops Prod* 222: 119501. https://doi.org/10.1016/j.indcrop.2024.119501
2. Elfaleh I, Abbassi F, Habibi M, et al. (2023) A comprehensive review of natural fibers and their composites: An eco-friendly alternative to conventional materials. *Results Eng* 19: 101271. https://doi.org/10.1016/j.rineng.2023.101271

3. Khan F, Hossain N, Mim JJ, et al. (2024) Advances of composite materials in automobile applications—A review. *J Eng Res* 13: 1001–1023. https://doi.org/10.1016/j.jer.2024.02.017
4. Karimah A, Ridho MR, Munawar SS, et al. (2021) A review on natural fibers for development of eco-friendly bio-composite: Characteristics, and utilizations. *J Mater Res Technol* 13: 2442–2458. https://doi.org/10.1016/j.jmrt.2021.06.014
5. Wagh J, Madgule M, Awadhani LV (2023) Investigative studies on the mechanical behavior of Jute, Sisal, Hemp, and glass fiber-based composite material. *Mater Today Proc* 77: 969–976. https://doi.org/10.1016/j.matpr.2022.12.101
6. Awais H, Nawab Y, Amjad A, et al. (2021) Environmental benign natural fibre reinforced thermoplastic composites: A review. *Composites Part C* 4: 100082. https://doi.org/10.1016/j.jcomc.2020.100082
7. Hasanuddin I, Mawardi I, Nurdin N, et al. (2023) Evaluation of properties of hybrid laminated composites with different fiber layers based on Coir/Al_2O_3 reinforced composites for structural application. *Results Eng* 17: 100948. https://doi.org/10.1016/j.rineng.2023.100948
8. Zaman HU, Beg MDH (2014) Preparation, structure, and properties of the coir fiber/polypropylene composites. *J Compos Mater* 48: 3293–3301. https://doi.org/10.1177/0021998313508996
9. Islam MN, Rahman MR, Haque MM, et al. (2010) Physico-mechanical properties of chemically treated coir reinforced polypropylene composites. *Compos Part A Appl Sci Manuf* 41: 192–198. https://doi.org/10.1016/j.compositesa.2009.10.006
10. Satyanarayana KG (1981) A review on sisal fiber reinforced polymer composites. *J Sci Ind Res* 40: 222–237. https://doi.org/10.1590/1807-1929/agriambi.v3n3p367-379
11. Karim MA, Abdullah MA, Deifalla AF, et al. (2023) An assessment of the processing parameters and application of fibre-reinforced polymers (FRPs) in the petroleum and natural gas industries: A review. *Results Eng* 18: 101091. https://doi.org/10.1016/j.rineng.2023.101091
12. Freitas BR, Braga JO, Orlandi MP, et al. (2022) Characterization of coir fiber powder (cocos nucifera L.) as an environmentally friendly inhibitor pigment for organic coatings. *J Mater Res Technol* 19: 1332–1342. https://doi.org/10.1016/j.jmrt.2022.05.098
13. Singh MK, Tewari R, Zafar S, et al. (2023) A comprehensive review of various factors for application feasibility of natural fiber-reinforced polymer composites. *Results Mater* 17: 100355. https://doi.org/10.1016/j.rinma.2022.100355
14. Moharana S, Sahu BB, Nayak AK, et al. (2024) *Polymer Composites: Fundamentals and Applications*, Singapore: Springer Singapore. https://doi.org/10.1007/978-981-97-2075-0
15. Wong D, Fabito G, Debnath S, et al. (2024) A critical review: Recent developments of natural fiber/rubber reinforced polymer composites. *Clean Mater* 13: 100261. https://doi.org/10.1016/j.clema.2024.100261
16. Thandavamoorthy R, Alagarasan JK, Mohanavel V, et al. (2024) Fabrication of kenaf fiber reinforced boron carbide fillers embedded epoxy matrix composite—An antimicrobial and structural analysis. *J Mater Res Technol* 33: 2560–2567. https://doi.org/10.1016/j.jmrt.2024.09.236
17. Srinivas A, Sreenivasa CG, Mahadev M (2024) A review on–Variants in specimen preparation of natural fiber composites. *AIP Conf Proc* 3013: 20013. https://doi.org/10.1063/5.0202052

18. Karthik K, Rajamanikkam RK, Venkatesan EP, et al. (2024) State of the art: Natural fibre-reinforced composites in advanced development and their physical/chemical/mechanical properties. *Chinese J Anal Chem* 52: 100415. https://doi.org/10.1016/j.cjac.2024.100415
19. Rampal, Kumar G, Rangappa SM, et al. (2022) A review of recent advancements in drilling of fiber-reinforced polymer composites. *Compos Part C-Open* 9: 100312. https://doi.org/10.1016/j.jcomc.2022.100312
20. Fallahi H, Kaynan O, Asadi A (2023) Insights into the effect of fiber–matrix interphase physiochemical-mechanical properties on delamination resistance and fracture toughness of hybrid composites. *Compos Part A Appl Sci Manuf* 166: 107390. https://doi.org/10.1016/j.compositesa.2022.107390
21. Slamani M, Joma W, Elhadi A, et al. (2024) Investigating the impact of drill material on hole quality in jute/palm fiber reinforced hybrid composite drilling with uncertainty analysis. *Heliyon* 10: 36925. https://doi.org/10.1016/j.heliyon.2024.e36925
22. Tamilvendan D, Ravikumar AR, Munimathan A (2024) Mechanical behavior of sisal glass-reinforced polymer composites under tensile loading and geometric irregularities. *Proc Inst Mech Eng Part E.* https://doi.org/10.1177/09544089241270770
23. Pérez-Salinas C, Castro-Miniguan C, Moya-Moya E, et al. (2023) Analysis of surface roughness and delamination factor applied to the drilling of hybrid polymeric composite materials by the Taguchi method. *Mater Today Proc*. https://doi.org/10.1016/j.matpr.2023.06.437
24. Bhosale R, Madgule M (2024) Optimization techniques for material selection and manufacturing processes: A review. *JMST Adv* 7: 57–68. https://doi.org/10.1007/s42791-024-00093-x
25. Ramnath BV, Sharavanan S, Jeykrishnan J (2017) Optimization of process parameters in drilling of fibre hybrid composite using Taguchi and grey relational analysis. *IOP Conf Ser Mater Sci Eng* 183: 012003. https://doi.org/10.1088/1757-899X/183/1/012003
26. Wasti S, Kamath D, Armstrong K (2024) Life cycle assessment of coir fiber-reinforced composites for automotive applications. *J Clean Prod* 485: 144368. https://doi.org/10.1016/j.jclepro.2024.144368
27. Alsuwait RB, Souiyah M, Momohjimoh I, et al. (2023) Recent development in the processing, properties, and applications of epoxy-based natural fiber polymer biocomposites. *Polymers* 15: 145. https://doi.org/10.3390/polym15010145
28. Madgule M, Deshmukh P, Perveen K, et al. (2023) Experimental investigation on mechanical properties of novel polymer hybrid composite with reinforcement of banana fiber and sugarcane bagasse powder. *Adv Mech Eng* 10: 15. https://doi.org/10.1177/16878132231203810
29. ASTM International (2017) Standard test method for tensile properties of polymer matrix composite materials. ASTM D3039/D3039M–17, West Conshohocken, PA. https://doi.org/10.1520/D3039_D3039M-17
30. Pathak SR, Malik A, Mali HS (2025) Experimental investigation on drilling behavior of carbon-Kevlar monolithic and interyarn hybrid composite. *Compos B Eng* 301: 112499. https://doi.org/10.1016/j.compositesb.2025.112499
31. Ghabezi P, Farahani M, Shahmirzaloo A, et al. (2019) Defect evaluation of the honeycomb structures formed during the drilling process. *Int J Damage Mech* 29: 454–466. https://doi.org/10.1177/1056789519860573

32. Khoran M, Ghabezi P, Farahani M (2014) Optimization of drilling process on corrugated-core sandwich panels. *Int J Adv Manuf Technol* 77: 1475–1483. https://doi.org/10.1007/s00170-014-6427-X

AIMS Press